Enhanced control of saddle steady states of dynamical systems

Arūnas Tamaševičius,[1,*] Elena Tamaševičiūtė,[1] Gytis Mykolaitis,[2] and Skaidra Bumelienė[1]

[1]*Department of Electronics, Center for Physical Sciences and Technology, LT-01108 Vilnius, Lithuania*
[2]*Department of Physics, Vilnius Gediminas Technical University, LT-10223 Vilnius, Lithuania*

An adaptive feedback technique for stabilizing *a priori* unknown saddle steady states of dynamical systems is described. The method is based on an unstable low-pass filter combined with a stable low-pass filter. The cutoff frequencies of both filters can be set relatively high. This allows considerable increase in the rate of convergence to the steady state. We demonstrate numerically and experimentally that the technique is robust to the influence of unknown external forces, which change the position of the steady state in the phase space. Experiments have been performed using electrical circuits imitating the damped Duffing-Holmes and chaotic Lindberg systems.

PACS number(s): 05.45.−a, 07.05.Dz, 84.30.−r

I. INTRODUCTION

A number of adaptive, that is model-independent and reference-free, feedback methods for controlling unstable states of dynamical systems have been proposed. An example is the derivative feedback technique [1,2], applied to stabilize a laser [1], and an electrochemical reaction [2]. Other examples are low-, high-, and all-pass filter methods [3–9]. The methods have been tested in several experimental systems, including electrical circuits [3,4,8] and lasers [5,6,9]. Two more methods, namely the time-delayed feedback method [10,11] and the notch-filter method [9,12,13], although originally designed to control chaotic systems, under appropriate set of parameters can be used to stabilize the steady states as well [13,14].

However, all the above-mentioned techniques, when applied to control steady states, are able to stabilize nodes and spirals only. They fail to control the saddle states, more precisely the states characterized with an odd number of real positive eigenvalues. To solve the problem of the odd number limitation, Pyragas *et al.* proposed to use an unstable filter [15,16]. It was an elegant idea to suppress one instability with another instability. The technique has been demonstrated to stabilize saddles in several mathematical models [15–17] also applied to experimental systems, e.g., an electrochemical oscillator [15,16] and the Duffing-Holmes electronic circuit [17]. The original unstable filter controller, however, works in the dissipative systems only. The controller has been extended to conservative systems, e.g., the Lagrange point L2 of the Sun-Earth system [18]. Here the situation is similar to the famous Ott-Grebogi-Yorke (OGY) method of controlling chaos [19], in the sense that it does not work in the Hamiltonian systems [20]. Another limitation of the original controller is its slow performance, especially when applied to weakly damped systems. It has been derived analytically from the Hurwitz criteria for a pendulum [16,17] and for the Duffing-Holmes oscillator [17] that the dimensionless cut-off frequency of the unstable filter ω should be set less than the dimensionless damping coefficient b. For small b, consequently small ω, the transients become very long [16,17]. Whereas the chaotic Lorenz system exhibits fast convergence to the stabilized saddle state [16], because the effective damping parameter

appears to be large ($b > 1$), as shown in Table I. In the previous works [15–17], the performance of the unstable filter controller is demonstrated for the installation stage (turn on for the first time). Specifically, the evolution from either the originally oscillatory and rotatory states [15,16] or from an originally stable steady state [17] to the saddle steady state is presented. Whereas, from a practical point of view, whenever the steady state is stabilized, the robustness of the system under the unknown external perturbations, which can change the coordinates of the steady state, is an important issue.

In this work, we describe an improved (enhanced) method for stabilizing saddle steady states and consider the response of the overall system (dynamical system plus controller) to the external *a priori* unknown force.

II. DYNAMICAL SYSTEMS WITH SADDLE STEADY STATES

We consider saddle steady states of five different physical systems. The first example is a pendulum given by

$$\ddot{\varphi} + \beta\dot{\varphi} + \sin\varphi = 0. \tag{1}$$

Here, φ is the angle between the downward vertical and the rod, and β is the damping parameter. Pendulum has two steady states $(\varphi_0,\dot{\varphi}_0)$: a stable spiral or a node (depending on β) at $(0,0)$ and a saddle at $(\pi,0)$.

The second example is the Duffing-Holmes damped oscillator [21]:

$$\ddot{x} + b\dot{x} + x^3 - x = 0. \tag{2}$$

Here, b is the damping coefficient. The oscillator has three steady states $(x_0,\dot{x})$: two symmetrical stable spirals or nodes (depending on b) at $(\pm 1,0)$ and a saddle at $(0,0)$.

The third example is a conservative astrodynamical system, namely a body at the Lagrange point L2 of the Sun-Earth system with no damping [18]:

$$\ddot{r} - \Omega^2 f(r) = 0, \quad \Omega^2 = \frac{\gamma M}{R_0^3},$$
$$f(r) = 1 + r - \frac{1}{(1+r)^2} - \frac{\varepsilon}{r^2}. \tag{3}$$

Here, $r = R/R_0$; R and R_0 are the distances of the Lagrange point L2 from the Earth and of the Earth from the Sun,

*tamasev@pfi.lt

TABLE I. Variables Q, P and parameters a, b of Eq. (6).

System	Q	P	a	b
Pendulum	φ	$\dot{\varphi}$	1	$\beta > 0$
Duffing-Holmes	x	$\dot{x}$	1	$b > 0$
Lagrange L2	r	$\dot{r}$	$\Omega^2 f'(r_0) > 0$	0
Lorenz	x	$-x + y$	$(r-1)/\sigma > 0$	$(\sigma+1)/\sigma$
Lindberg	x	$\dot{x}$	$1 - c\omega_c > 0$	$-b < 0$

respectively; γ is the gravitational constant; m and M are the masses of the Earth and the Sun, respectively; $\varepsilon = m/M \approx 3.10^{-6}$. The system has a single steady state $[r_0, \dot{r}] = [(\varepsilon/3)^{1/3}, 0]$, which is a saddle.

The fourth example is the the third order chaotic Lorenz system [21]

$$\dot{x} = -\sigma x + \sigma y, \tag{4a}$$
$$\dot{y} = -xz + rx - y, \tag{4b}$$
$$\dot{z} = xy - bz. \tag{4c}$$

Here σ, r, and b are fixed positive parameters. The Lorenz system at $r > 1$ has three steady states, a saddle at the origin $(0,0,0)$ and two symmetrical stable spirals $(\pm\sqrt{b(r-1)}, \pm\sqrt{b(r-1)}, r-1)$. For $r > r_{\text{th}} = \sigma(\sigma + b + 3)/(\sigma - b - 1)$, the spirals become unstable giving rise to chaotic oscillations. For common parameter values $\sigma = 10$ and $b = 8/3$ the $r_{\text{th}} \approx 24.7$.

The fifth example is the Lindberg oscillator [22]:

$$\ddot{x} - b\dot{x} + x^3 - x + cz = 0, \tag{5a}$$
$$\dot{z} = \omega_c(\dot{x} - z). \tag{5b}$$

In contrast to the Duffing-Holmes damped oscillator, the Lindberg oscillator has a negative damping term $-b\dot{x}$ in Eq. (5a), which makes it oscillating, whereas Eq. (5b) results in chaotic oscillations. In Eq. (5), the $c \approx 1$ and $\omega_c < 1$ [22]. The Lindberg oscillator has three steady states $(x_0, \dot{x}_0, z_0)$: two symmetrical unstable spirals or nodes (depending on b) $(\pm 1, 0, 0)$ and a saddle at the origin $(0,0,0)$.

When linearized around the saddle steady states, all the above systems have a simple common form:

$$\dot{Q} = P, \tag{6a}$$
$$\dot{P} = aQ - bP, \tag{6b}$$

where the generalized variables Q, P and parameters a, b are presented in Table I.

Though the Lorenz system is a set of three equations, the linearized set ($x_0 = y_0 = z_0$) becomes partially decoupled:

$$\dot{x} = -\sigma x + \sigma y, \tag{7a}$$
$$\dot{y} = rx - y, \tag{7b}$$
$$\dot{z} = -bz, \tag{7c}$$

that is the third equation, Eq. (7c) for z contains neither x nor y. Consequently, dynamics of the Lorenz system near the saddle point can be described by the second-order linear system. Note that to obtain the common form [Eq. (6)] the following linear transformations $\sigma t \to t$ and $P = -x + y$ have been applied to the linearized Lorenz equations. Therefore, the new variable P and parameters a,b in Table I for the Lorenz

system are combinations of the original variables x, y and r, σ, respectively.

A somewhat different situation is with the Lindberg oscillator at the origin $x_0 = \dot{x}_0 = z_0 = 0$. In this case, Eq. (5b) remains coupled via the $\dot{x}$ variable. However, because of $\omega_c < 1$ dynamics of the z variable is relatively slow and Eq. (5b) can be reduced to $\dot{z} \approx \omega_c \dot{x}$ and $z \approx \omega_c x$. Then the dynamics of the Lindberg oscillator near the saddle point can be approximated by Eq. (6) with an effective parameter $a \approx 1 - c\omega_c$.

III. UNSTABLE FILTER METHOD

In this section, we demonstrate the limitations of unstable filter method used for controlling saddle steady states. Equations (6) with the control term $k(u - Q)$ and the additional equation of the unstable filter for variable u read

$$\dot{Q} = P, \tag{8a}$$
$$\dot{P} = aQ - bP + k(u - Q), \tag{8b}$$
$$\dot{u} = \omega(u - Q). \tag{8c}$$

The corresponding characteristic equation is

$$\lambda^3 + (b - \omega)\lambda^2 + (k - a - \omega b)\lambda + a\omega = 0. \tag{9}$$

The overall system is stable if the real parts of all three eigenvalues of Eq. (9) are negative. The necessary and sufficient conditions can be found from the Hurwitz matrix:

$$H_3 = \begin{pmatrix} b - \omega & \omega & 0 \\ 1 & k - a - b\omega & 0 \\ 0 & b - \omega & a\omega \end{pmatrix}.$$

The eigenvalues $\text{Re}\lambda_{1,2,3}$ are all negative if the diagonal minors of the H_3 matrix are all positive:

$$\Delta_1 = b - \omega > 0, \tag{10a}$$
$$\Delta_2 = (b - \omega)(k - a - b\omega) - \omega > 0, \tag{10b}$$
$$\Delta_3 = a\omega\Delta_2 > 0. \tag{10c}$$

These inequalities are satisfied if

$$\omega < b, \tag{11a}$$
$$k > k_{\text{th}} = a + \frac{\omega}{b - \omega} + b\omega. \tag{11b}$$

For example, at $a = 1$, $b = 0.1$, and $\omega = 0.02$ the $k_{\text{th}} = 1.252$. On one hand, according to the inequality Eq. (11a), the ω could be only slightly less than b. On the other hand, it should not be too close to b, because small value of the denominator $b - \omega$ in the inequality Eq. (11b) would heavily increase the stabilization threshold k_{th}.

Numerical solution of the characteristic equation is plotted in Fig. 1. The largest eigenvalues $\text{Re}\lambda_1 = \text{Re}\lambda_2$ cross zero axis at $k \approx 1.25$ in a good agreement with the analytical result. We note very small absolute values of the largest $\text{Re}\lambda_{\text{max}}$ at $k > k_{\text{th}}$. In the full scale [Fig. 1(a)], the dots lay almost on the zero axis. Only the zoomed in plot [Fig. 1(b)] clearly reveals the negative values. However, even at $k = k_{\text{opt}} = 1.7$ the $|\text{Re}\lambda_{\text{max}}| = 0.025$. Such a low value, related to small parameters b and ω, results in slow convergence (long transients) to the steady state. This is a serious shortcoming of the unstable filter method, especially if applied to weakly damped ($b \leqslant 0.1$) dynamical systems.
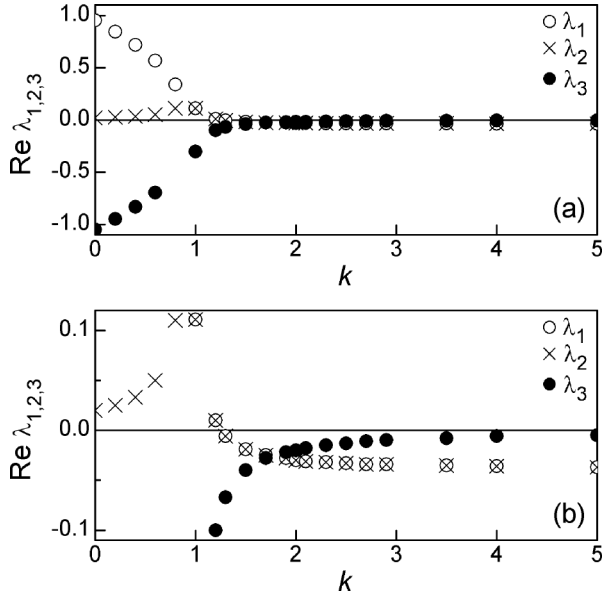
FIG. 1. Real parts of the eigenvalues $\mathrm{Re}\lambda_{1,2,3}$ versus the control gain k from Eq. (9) with $a = 1$, $b = 0.1$, $\omega = 0.02$. (a) Full scale. (b) Vertically zoomed in scale.

Now we present numerical results (Fig. 2) of the control dynamics under the influence of an *a priori* unknown external constant force p, which changes the position of the saddle steady state. To be specific, we consider the Duffing-Holmes nonlinear system [Eq. (2)] given in the following form:

$$\dot{x} = y, \tag{12a}$$
$$\dot{y} = x - x^3 - by + k(u - x) + p, \tag{12b}$$
$$\dot{u} = \omega(u - x). \tag{12c}$$

At $t < 50$ the saddle steady state $(0;0)$ is stabilized. The external force $p = -0.3$ applied at $t \geqslant 50$ changes the coordinates of the steady state from $(0;0)$ to $(0.34;0)$. After some transient process, the controller stabilizes the new steady state. The transients are sufficiently short for large b [Fig. 2(a)]. However, for smaller b they become extremely long [Fig. 2(c)]. Moreover, before settling on the new steady state ($+0.34$), the x variable, even for heavy damping ($b = 1$), exhibits undesirably deep negative drop (-0.3), while for weak damping ($b = 0.1$) the drop is (-0.5).

IV. ENHANCED FILTER METHOD

We suggest the following modification of the unstable filter method to improve its performance:

$$\dot{Q} = P, \tag{13a}$$
$$\dot{P} = aQ - bP + k_1(u - Q) + k_2(v - Q), \tag{13b}$$
$$\dot{u} = \omega_1[(u - Q) + k_2(v - Q)], \tag{13c}$$
$$\dot{v} = \omega_2(Q - v). \tag{13d}$$

Here, the unstable filter given by Eq. (13c) is combined with a stable one described by Eq. (13d), whereas the control force in Eq. (13b) consists of two terms, $k_1(u - Q)$ and $k_2(v - Q)$.
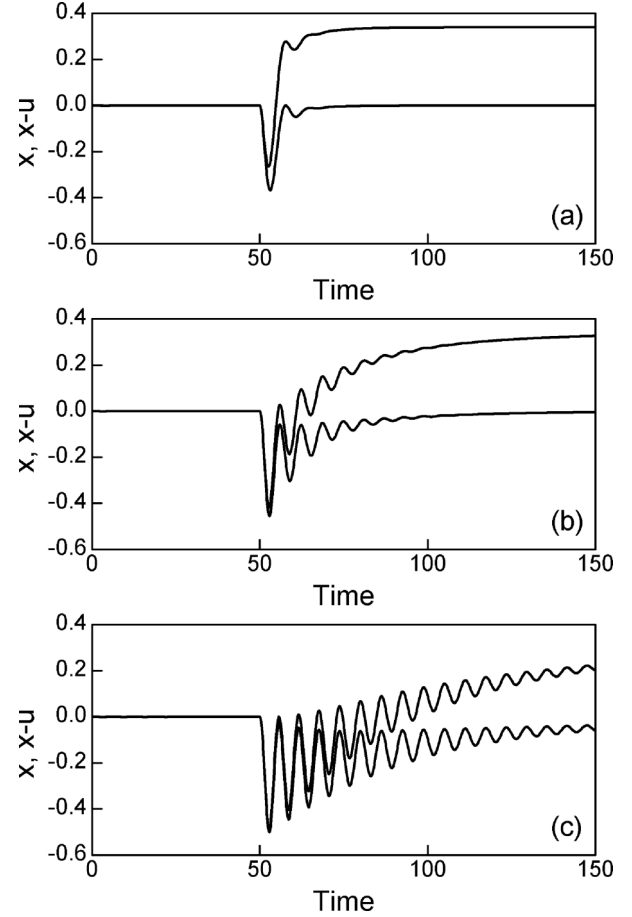
FIG. 2. Controlling the saddle in the Duffing-Holmes system from Eq. (12). $k = 2$. (a) $b = 1$, $\omega = 0.2$. (b) $b = 0.3$, $\omega = 0.06$. (c) $b = 0.1$, $\omega = 0.02$. Upper traces, variable x; lower traces, inverted control term $-k(u - x)/2 = (x - u)$.

Correspondingly, the characteristic equation is

$$\lambda^4 + (\omega_2 - \omega_1 + b)\lambda^3$$
$$+ [k_1 + k_2 - a - \omega_1\omega_2 + b(\omega_2 - \omega_1)]\lambda^2$$
$$+ [(k_1 - a)\omega_2 - (k_2 - a)\omega_1 - b\omega_1\omega_2 + k_1k_2\omega_1]\lambda$$
$$+ a\omega_1\omega_2 = 0. \tag{14}$$

The Hurwitz matrix is

$$H_4 = \begin{pmatrix} a_1 & a_3 & 0 & 0 \\ 1 & a_2 & a_4 & 0 \\ 0 & a_1 & a_3 & 0 \\ 0 & 1 & a_2 & a_4 \end{pmatrix},$$

with its elements

$$a_1 = \omega_2 - \omega_1 + b,$$
$$a_2 = k_1 + k_2 - a - \omega_1\omega_2 + b(\omega_2 - \omega_1),$$
$$a_3 = (k_1 - a)\omega_2 - (k_2 - a)\omega_1 - b\omega_1\omega_2 + k_1k_2\omega_1,$$
$$a_4 = a\omega_1\omega_2. \tag{15}$$

The diagonal minors of the H_4 matrix are the following:

$$\Delta_1 = a_1 = \omega_2 - \omega_1 + b > 0, \tag{16a}$$

$$\begin{aligned}\Delta_2 &= a_1 a_2 - a_3 \\ &= \omega_2 k_2 - \omega_1 k_1 - (\omega_2 - \omega_1)\omega_1 \omega_2 \\ &\quad + b(\omega_2 - \omega_1)^2 + b^2(\omega_2 - \omega_1) \\ &\quad + b(k_1 + k_2 - a) - k_1 k_2 \omega_1 > 0, \end{aligned} \tag{16b}$$

$$\Delta_3 = a_3 \Delta_2 - a_1^2 a_4 > 0, \tag{16c}$$

$$\Delta_4 = a_4 \Delta_3 > 0. \tag{16d}$$

Inequality Eq. (16a) is satisfied if

$$\omega_2 > \omega_1 - b. \tag{17}$$

For small b, inequality Eq. (17) reads $\omega_2 > \omega_1$. It means that, in contrast to the simple unstable filter method, this stability criterion does not depend on the system parameters but can be fully satisfied by the controller parameters.

For $\omega_2 \gg \omega_1$ and $0 < b \ll 1$, the threshold gain $k_{2\text{th}}$ can be roughly estimated from inequality Eq. (16b):

$$k_2 > k_{2\text{th}} \approx \frac{\omega_1 \omega_2^2}{\omega_2 - k_1 \omega_1}. \tag{18}$$

For example, at $k_1 = 2$, $\omega_1 = 1$, and $\omega_2 = 5$ the $k_{2\text{th}} \approx 8.3$. In Eq. (16d), the $\Delta_4 > 0$, if $\Delta_3 > 0$, since $a_4 > 0$. However, analysis of the minor Δ_3 is very complicated. Therefore, we employ the numerical solutions of the characteristic equation, which are presented in Fig. 3.

Similar to Sec. III, we consider the Duffing-Holmes system with the external force p, but now with two combined filters and two control terms in the feedback:

$$\dot{x} = y, \tag{19a}$$

$$\dot{y} = x - x^3 - by + k_1(u - x) + k_2(v - x) + p \tag{19b}$$

$$\dot{u} = \omega_1[(u - x) + k_2(v - x)], \tag{19c}$$

$$\dot{v} = \omega_2(x - v). \tag{19d}$$
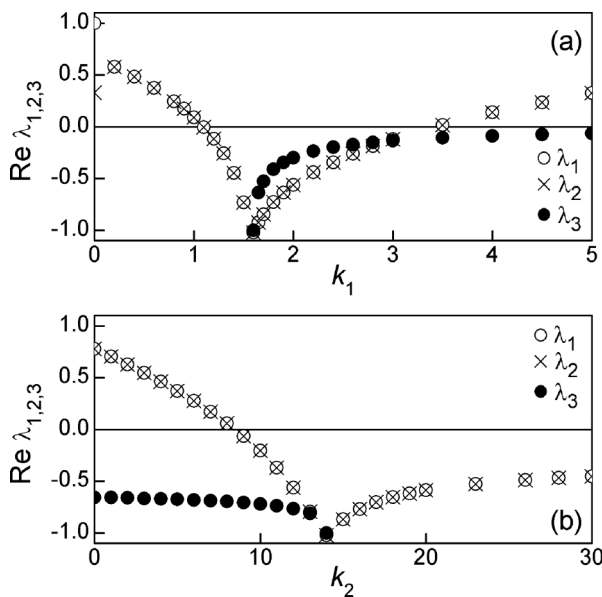
FIG. 3. Real parts of the eigenvalues $\mathrm{Re}\lambda_{1,2,3}$ versus the control gains k_1 and k_2 from Eq. (14). $a = 1$, $b = 0.1$, $\omega_1 = 1$, $\omega_2 = 5$. (a) $k_2 = 14$. (b) $k_1 = 1.6$. The $\mathrm{Re}\lambda_4 < -1$ is not plotted.
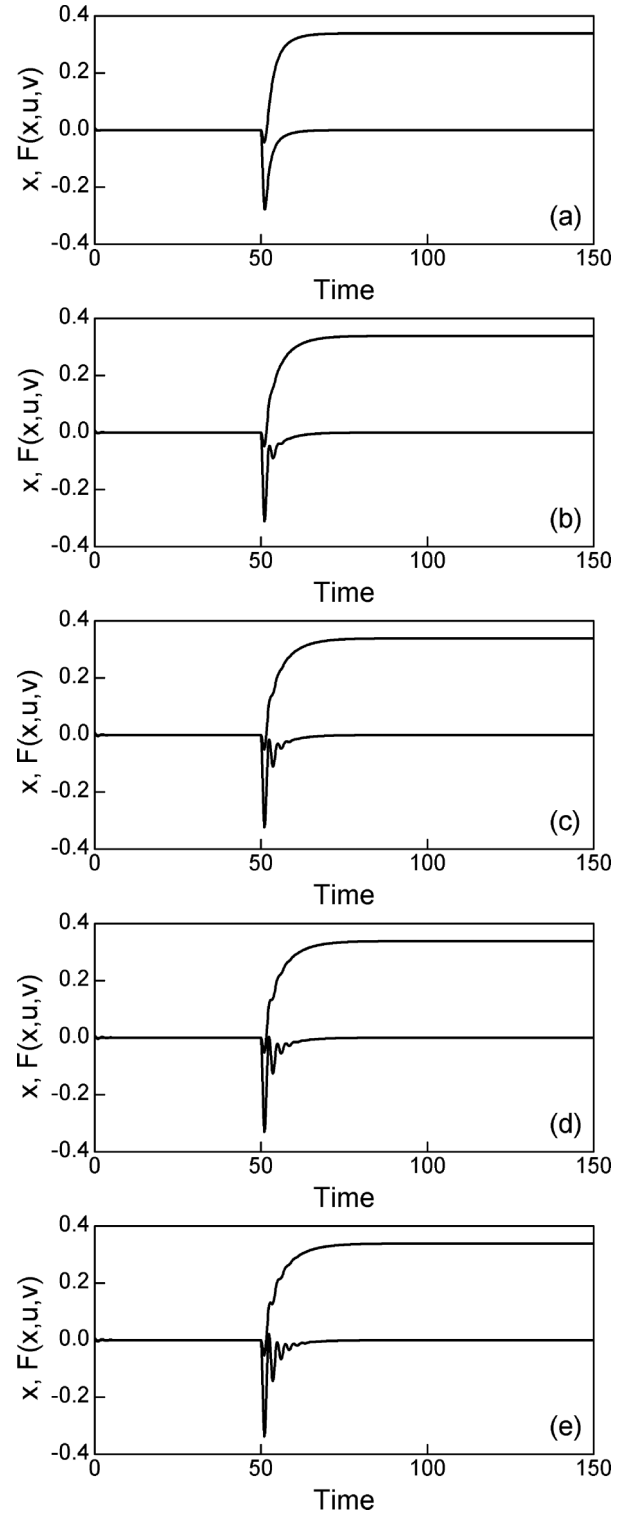
FIG. 4. Controlling the saddle in the Duffing-Holmes system from Eq (19). $k_1 = 2$, $k_2 = 14$, $\omega_1 = 1$, $\omega_2 = 5$. (a) $b = 1$. (b) $b = 0.3$. (c) $b = 0.1$. (d) $b = 0$. (e) $b = -0.1$. Upper traces, variable x; lower traces, inverted control term $F(x,u,v) = -[k_1(u - x) + k_2(v - x)]/2$.

The results are shown in Fig. 4. There are two main differences in comparison with the simple unstable filter technique (Fig. 2). First, the transients are essentially shorter. Second, the negative
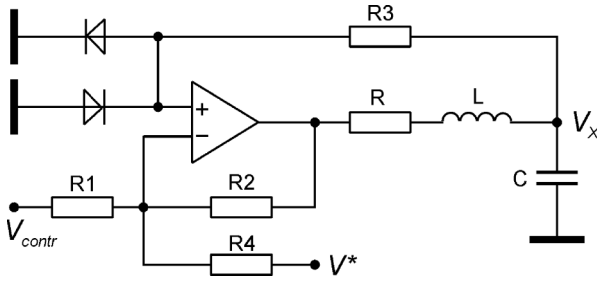
FIG. 5. Duffing-Holmes oscillator. V_{contr} is control voltage; V^* is external perturbation voltage.

FIG. 7. Enhanced filter controller. $V_{\text{in}} = V_x$.

drop of the x variable is only -0.04, which is more than 10 times smaller than in the case of the simple unstable filter. In addition, the enhanced filter technique is capable of stabilizing saddle steady states in conservative systems ($b = 0$) and active oscillators with negative damping ($b < 0$).

V. EXPERIMENTAL

A. Duffing-Holmes damped oscillator

Circuit diagram of the Duffing-Holmes oscillator is sketched in Fig. 5. The circuit element values are the following: $R_1 = R_2 = R_3 = 10$ kΩ, $R_4 = 1$ MΩ, R is specified in the corresponding figure captions, $L = 19$ mH, $C = 470$ nF. Operational amplifier is the LM741 or similar integrated circuit. Diodes are the N4148 or similar devices. Actually, it is a simplified version of the low-frequency Young-Silva oscillator [23]. The simplified circuit has been used previously to demonstrate switching from a stable spiral to the saddle point [17] also to demonstrate chaos control in a nonautonomous (periodically driven) Duffing-Holmes system by means of the time-delayed feedback [24] and the extended resonant feedback [25].

B. Unstable filter controller

Circuit diagram of the unstable filter controller is shown in Fig. 6. The circuit elements are: $R_1 = 9.1$ kΩ, C_1 is an adjustable value; see caption to Fig. 8. Instrumentation amplifiers IA1 and IA2 are the AD620-type integrated circuits with $k_{01} = 1$ and $k_{02} = 2$, respectively.

C. Enhanced filter controller

Circuit diagram of the enhanced filter controller is presented in Fig. 7. The nominal values of the circuit elements are the
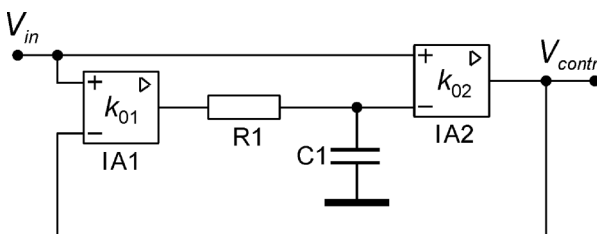
FIG. 6. Unstable filter controller. $V_{\text{in}} = V_x$.
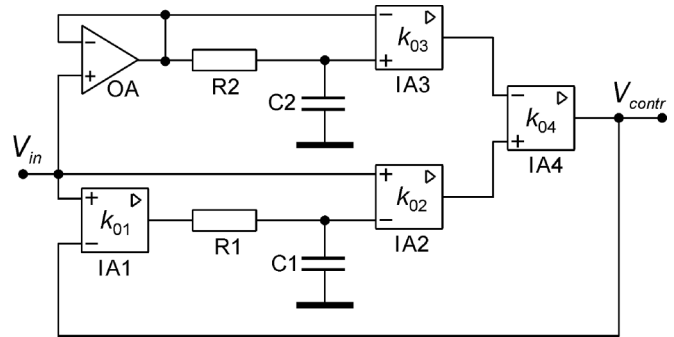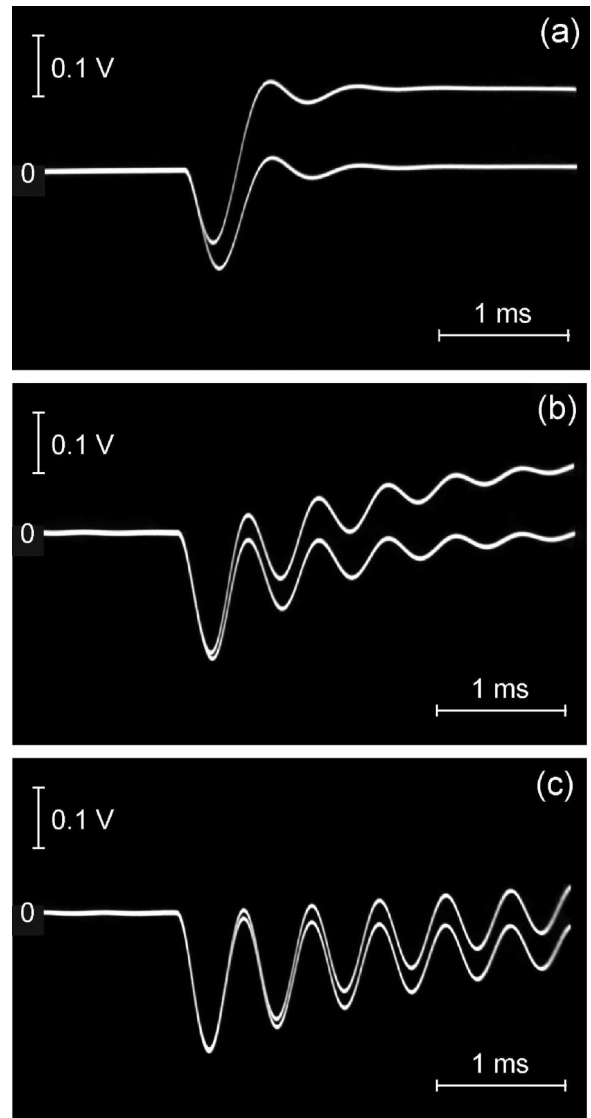
FIG. 8. Controlling the saddle in the Duffing-Holmes oscillator. External perturbation $V^* = 15$ V. (a) $R = 200$ Ω ($b = 1$), $C_1 = 51$ nF ($\omega = 0.2$). (b) $R = 60$ Ω ($b = 0.3$), $C_1 = 175$ nF ($\omega = 0.06$). (c) $R = 20$ Ω ($b = 0.1$), $C_1 = 510$ nF ($\omega = 0.02$. Upper traces, output signal of the oscillator V_x; lower traces, control signal $V_{\text{contr}}/2$.
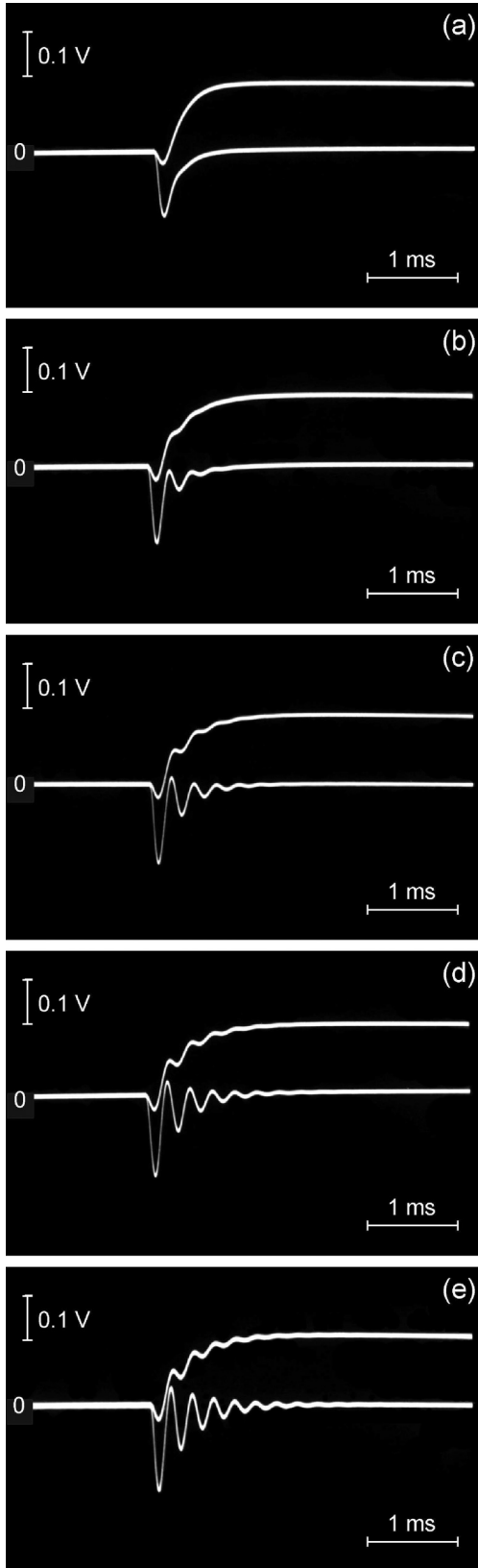
FIG. 9. Controlling the saddle in the Duffing-Holmes oscillator. External perturbation $V^* = 15$ V. (a) $R = 200$ Ω ($b = 1$). (b) $R = 60\Omega$ ($b = 0.3$). (c) $R = 20$ Ω ($b = 0.1$). (d) $R = r = 2$ Ω ($b = 0.01 \approx 0$). (e) $R_{eff} = -20$ Ω ($b = -0.1$). Upper traces, output signal of the oscillator V_x; lower traces, control signal $V_{contr}/2$.

following: $R_1 = R_2 = 9.1$ kΩ, $C_1 = 10$ nF, $C_2 = 2$ nF ($\omega_1 = \sqrt{LC}/R_1C_1$, $\omega_2 = \sqrt{LC}/R_2C_2 = 5$). Operational amplifier OA is the LM741-type or similar integrated circuit. Instrumentation amplifiers IA1, IA2, and IA4 are the AD620-type, and IA3 is the AD627-type integrated circuit, respectively. The $k_{01} = k_{02} = 1$, $k_{03} = 7$, $k_{04} = 2$. The $k_1 = k_{02}k_{04} = 2$ and the $k_2 = k_{03}k_{04} = 14$.

D. Experimental results

Experimental results presented in Figs. 8 and 9 coincide very well with the numerical simulations shown in Figs. 2 and 4, respectively. To implement the "zero" damping ($b \approx 0$) in Fig. 9(d) we have removed in the circuit (Fig. 5) the series resistor R; the remaining resistance is $R = r = 2$ Ω only, where r is the internal resistance of the inductive coil L. Whereas, the negative damping [Fig. 9(e)] is introduced in the system (with $R = 20$ Ω) by means of coupling a negative resistance $R_N = -1$ kΩ in parallel to the capacitor C. The negative resistance R_N is implemented using a negative impedance converter [26]. The resulting effective resistance in the series RLC circuit is $R_{eff} = -20$ Ω. This is not a full circuit of the Lindberg oscillator [22], since it lacks the inertial subcircuit described by Eq. (5b). However, it reflects the properties of a saddle state in a system with a negative damping.

VI. CONCLUSIONS

We have proposed an adaptive control method for stabilizing *a priori* unknown saddle steady states of dynamical systems. The controller is model-independent and reference-free. It does not require knowledge of either the mathematical model or the position of the steady state, but automatically tracks the state and stabilizes it. The only feature to be known in advance is that the steady state is a saddle-type state. The numerical and experimental results have been presented for the Duffing-Holmes oscillator only. However, the common forms given by Eqs. (6), (8), and (13), as well as their subsequent mathematical analysis, indicate that the technique can be applied to many other dynamical systems having unstable saddle-type steady states (not only the specific systems listed in Table I). The suggested controller is essentially faster than the simple unstable filter-based version [15–17]. It is suitable to stabilize saddle steady states also in dynamical system with zero and negative damping. In contrast to the usual unstable filter technique, the parameters of the enhanced controller (the cutoff frequencies of the filters) can be set relatively high and are independent on the damping parameters of the dynamical system. The enhanced controller exhibits robust performance in the presence of external unknown forces, which change the coordinates of the steady state in the phase space. It tracks the position of the new saddle steady states and rapidly stabilizes them.

[1] S. Bielawski, M. Bouazaoui, D. Derozier, and P. Glorieux, Phys. Rev. A **47**, 3276 (1993).

[2] P. Parmananda, M. A. Rhode, G. A. Johnson, R. W. Rollins, H. D. Dewald, and A. J. Markworth, Phys. Rev. E **49**, 5007 (1994).

[3] N. F. Rulkov, L. S. Tsimring, and H. D. I. Abarbanel, Phys. Rev. E **50**, 314 (1994).

[4] A. Namajūnas, K. Pyragas, and A. Tamaševičius, Int. J. Bif. Chaos **7**, 957 (1997).

[5] M. Ciofini, A. Labate, R. Meucci, and M. Galanti, Phys. Rev. E **60**, 398 (1999).

[6] A. Schenck zu Schweinsberg and U. Dressler, Phys. Rev. E **63**, 056210 (2001).

[7] D. J. Braun, Phys. Rev. E **78**, 016213 (2008).

[8] R. Meucci, S. Euzzor, A. Geltrude, K. Al-Naimee, S. De Nicola, and F. T. Arecchi, Phys. Lett. A **376**, 834 (2012).

[9] A. Geltrude, K. Al-Naimee, S. Euzzor, R. Meucci, F. T. Arecchi, and B. K. Goswami, Commun Nonlinear Sci. Numer. Simul. **17**, 3031 (2012).

[10] K. Pyragas, Phys. Lett. A **170**, 421 (1992).

[11] K. Pyragas and A. Tamaševičius, Phys. Lett. A **180**, 99 (1993).

[12] R. Meucci, M. Ciofini, and R. Abbate, Phys. Rev. E **53**, R5537 (1996).

[13] A. Ahlborn and U. Parlitz, Phys. Rev. Lett. **96**, 034102 (2006).

[14] K. Pyragas, Phys. Lett. A **206**, 323 (1995).

[15] K. Pyragas, V. Pyragas, I. Z. Kiss, and J. L. Hudson, Phys. Rev. Lett. **89**, 244103 (2002).

[16] K. Pyragas, V. Pyragas, I. Z. Kiss, and J. L. Hudson, Phys. Rev. E **70**, 026215 (2004).

[17] A. Tamaševičius, E. Tamaševičiūtė, G. Mykolaitis, and S. Bumelienė, Phys. Rev. E **78**, 026205 (2008).

[18] A. Tamaševičius, E. Tamaševičiūtė, G. Mykolaitis, S. Bumelienė, and R. Kirvaitis, Phys. Rev. E **82**, 026205 (2010).

[19] E. Ott, C. Grebogi, and J. A. Yorke, Phys. Rev. Lett. **64**, 1196 (1990).

[20] Y.-Ch. Lai, M. Ding, and C. Grebogi, Phys. Rev. E **47**, 86 (1993).

[21] E. Ott, *Chaos in Dynamical Systems* (Cambridge University Press, Cambridge, 1993).

[22] E. Lindberg, E. Tamaševičiūtė, G. Mykolaitis, S. Bumelienė, T. Pyragienė, A. Tamaševičius, and R. Kirvaitis, in *Circuit Theory and Design*, Proc. Eur. Conf. (IEEE, Piscataway, NJ, 2009), p. 663, http://ieeexplore.ieee.org/hpl/articleDetails.jsp?arnumber=5275062.

[23] Y.-Ch. Lai, A. Kandangath, S. Krishnamoorthy, J. A. Gaudet, and A. P. S. de Moura, Phys. Rev. Lett. **94**, 214101 (2005).

[24] A. Tamaševičius, G. Mykolaitis, V. Pyragas, and K. Pyragas, Phys. Rev. E **76**, 026203 (2007).

[25] A. Tamaševičius, E. Tamaševičiūtė, T. Pyragienė, G. Mykolaitis, and S. Bumelienė, Commun. Nonlinear Sci. Numer. Simul. **14**, 4273 (2009).

[26] P. Horowitz and W. Hill, *The Art of Electronics* (Cambridge University Press, Cambridge, 1993).